V International Conference on Computational Methods in Marine Engineering
MARINE 2013
B. Brinkmann and P. Wriggers (Eds)

FAST SOLVERS FOR THERMAL FLUID STRUCTURE INTERACTION

PHILIPP BIRKEN*, TOBIAS GLEIM†, DETLEF KUHL† AND ANDREAS MEISTER*

*Institute of Mathematics
University of Kassel
Heinrich-Plett-Str. 40, 34132 Kassel, Germany
e-mail: {birken,meister}@mathematik.uni-kassel.de, web page:
http://www.mathematik.uni-kassel.de/

† Institute of Mechanics and Dynamics,
University of Kassel
Mönchebergstr. 7, 34109 Kassel, Germany
e-mail: {tgleim,kuhl}@uni-kassel.de - Web page: http://www.uni-kassel.de

Key words: Thermal Fluid Structure Interaction, Partitioned Coupling, Fixed Point methods, Vector Extrapolation

Abstract. We consider thermal fluid structure interaction to model industrial gas quenching in steel forging, where hot steel is cooled using cold high pressured gas. This allows to define properties of the finished steel part, as for example yield strength, locally at low cost and without environmental problems.

For the numerical simulation, a partitioned approach via a Dirichlet-Neumann coupling and a fixed point iteration is employed. In time, previously developed efficient time adaptive higher order time integration schemes are used. The respective models are the compressible Navier-Stokes equations and the nonlinear heat equation, where the parameter functions are obtained from measurements on a specific steel.

Here, the use of different vector extrapolation methods for convergence acceleration techniques of the fixed point iteration is analyzed. In particular, Aitken relaxation, minimal polynomial extrapolation (MPE) and reduced rank extrapolation (RRE) are considered.

1 INTRODUCTION

Thermal interaction between fluids and structures plays an important role in many applications. Examples for this are cooling of gas-turbine blades, thermal anti-icing systems of airplanes [3] or supersonic reentry of vehicles from space [12, 8]. Another is quenching,

an industrial heat treatment of metal workpieces. There, the desired material properties are achieved by rapid cooling, which causes solid phase changes, allowing to create graded materials with precisely defined properties.

Gas quenching recently received a lot of industrial and scientific interest [19, 7]. In contrast to liquid quenching, this process has the advantage of minimal environmental impact because of non-toxic quenching media and clean products like air [17]. Furthermore it is possible to control the cooling locally and temporally for best product properties and to minimize distortion by means of adapted jet fields, see [15].

To exploit the multiple advantages of gas quenching the application of computational fluid dynamics has proved essential [1, 17, 11]. Thus, we consider the coupling of the compressible Navier-Stokes equations as a model for air, along a non-moving boundary with the heat equation as a model for the temperature distribution in steel.

For the solution of a coupled problem, we use a partitioned approach [4], where different codes for the sub-problems are used and the coupling is done by a master program which calls interface functions of the other codes. This allows to use existing software for each sub-problem, in contrast to a monolithic approach, where a new code is tailored for the coupled equations. To satisfy the boundary conditions at the interface, the subsolvers are iterated in a fixed point procedure.

A fast solver is obtained by making use of a time adaptive higher order time integration method suggested in [2]. Namely, the singly diagonally implicit Runge-Kutta (SDIRK) method SDIRK2 is employed. Furthermore, it is imperative to reduce the number of fixed point iterations. Various methods have been proposed to increase the convergence speed of the fixed point iteration by decreasing the interface error between subsequent steps, for example Relaxation [10, 9], Interface-GMRES [13] or ROM-coupling [18]. Here, we consider Aitken Relaxation and two variants of polynomial vector extrapolation, namely MPE and RRE [16]. These are compared on the basis of the flow past a flat plate, basic test case for thermal fluid structure interaction.

2 GOVERNING EQUATIONS

The basic setting we are in is that on a domain $\Omega_1 \subset \mathbb{R}^d$ the physics is described by a fluid model, whereas on a domain $\Omega_2 \subset \mathbb{R}^d$, a different model describing a structure is used. The two domains are almost disjoint in that they are connected via an interface. The part of the interface where the fluid and the structure are supposed to interact is called the coupling interface $\Gamma \subset \partial\Omega_1 \cup \partial\Omega_2$. Note that Γ might be a true subset of the intersection, because the structure could be insulated. At the coupling interface Γ, coupling conditions are prescribed that model the interaction between fluid and structure. For the thermal coupling problem, these conditions are that temperature and the normal component of the heat flux are continuous across the interface.

We model the fluid using the Navier-Stokes equations, which are a second order system of conservation laws (mass, momentum, energy) modeling viscous compressible flow. We consider the two dimensional case, written in conservative variables density ρ, momentum

$\mathbf{m} = \rho\mathbf{v}$ and energy per unit volume ρE:

$$\begin{aligned} \partial_t \rho + \nabla \cdot \mathbf{m} &= 0, \\ \partial_t m_i + \sum_{j=1}^{2} \partial_{x_j}(m_i v_j + p\delta_{ij}) &= \frac{1}{Re}\sum_{j=1}^{2} \partial_{x_j} S_{ij}, \qquad i = 1,2, \\ \partial_t(\rho E) + \nabla \cdot (H\mathbf{m}) &= \frac{1}{Re}\sum_{j=1}^{2} \partial_{x_j}\left(\sum_{i=1}^{2} S_{ij} v_i - \frac{1}{Pr} q_j\right). \end{aligned}$$

Here, $\mathbf{S}$ represents the viscous shear stress tensor and $\mathbf{q}$ the heat flux. As the equation are dimensionless, the Reynolds number Re and the Prandtl number Pr appear. The equations are closed by the equation of state for the pressure $p = (\gamma - 1)\rho e$. Additionally, we prescribe appropriate boundary conditions at the boundary of Ω_1 except for Γ.

Regarding the structure model, we will consider heat conduction only. For steel, we have temperature-dependent and highly nonlinear specific heat capacity c_p and heat conductivity λ. Thus, we have the nonlinear heat equation for the structure temperature $\Theta(\mathbf{x}, t)$

$$\rho(\mathbf{x}) c_p(\Theta) \frac{d}{dt}\Theta(\mathbf{x}, t) = -\nabla \cdot \mathbf{q}(\mathbf{x}, t), \tag{1}$$

where

$$\mathbf{q}(\mathbf{x}, t) = -\lambda(\Theta)\nabla\Theta(\mathbf{x}, t)$$

denotes the heat flux vector. Here, we use coefficient functions that have been suggested in [14] to model the steel 51CrV4 and are given by

$$\lambda(\Theta) = 40.1 + 0.05\Theta - 0.0001\Theta^2 + 4.9 \cdot 10^{-8}\Theta^3 \tag{2}$$

and

$$c_p(\Theta) = -10 \ln\left(\frac{e^{-c_{p1}(\Theta)/10} + e^{-c_{p2}(\Theta)/10}}{2}\right) \tag{3}$$

with

$$c_{p1}(\Theta) = 34.2 e^{0.0026\Theta} + 421.15 \tag{4}$$

and

$$c_{p2}(\Theta) = 956.5 e^{-0.012(\Theta - 900)} + 0.45\Theta. \tag{5}$$

For the mass density $\rho = 7836\ \mathrm{kg/m^3}$. Finally, on the boundary, we have Neumann conditions $\mathbf{q}(\mathbf{x}, t) \cdot \mathbf{n}(\mathbf{x}) = q_b(\mathbf{x}, t)$.

3 DISCRETIZATION

3.1 Discretization in space

Following the partitioned coupling approach, we discretize the two models separately in space. For the fluid, we use a finite volume method, leading to

$$\frac{d}{dt}\mathbf{u} + \underline{\mathbf{h}}(\mathbf{u}, \mathbf{\Theta}) = \mathbf{0}, \tag{6}$$

where $\underline{\mathbf{h}}(\mathbf{u}, \mathbf{\Theta})$ represents the spatial discretization and its dependence on the temperatures in the fluid. In particular, the DLR TAU-Code is employed [5], which is a cell-vertex-type finite volume method with AUSMDV as flux function and a linear reconstruction.

Regarding structural mechanics, the use of finite element methods is ubiquitious. Therefore, we will also follow that approach here and use quadratic finite elements, leading to the nonlinear equation for all unknowns on Ω_2

$$\mathbf{M}(\mathbf{\Theta})\frac{\mathbf{d}}{\mathbf{dt}}\mathbf{\Theta}(\mathbf{x}, \mathbf{t}) + \mathbf{K}(\mathbf{\Theta})\mathbf{\Theta}(\mathbf{x}, \mathbf{t}) = \mathbf{q_b}(\mathbf{x}, \mathbf{t}). \tag{7}$$

Here, $\mathbf{M}$ is the heat capacity and $\mathbf{K}$ the heat conductivity matrix. The vector $\mathbf{\Theta}$ consists of all discrete temperature unknowns and $\mathbf{q}_b(\mathbf{x}, t)$ is the heat flux vector on the surface. In this case it is the prescribed Neumann heat flux vector of the fluid.

3.2 Coupled time integration

If the fluid and the solid solver are able to carry out time steps of implicit Euler type, the master program of the FSI procedure can be extended to SDIRK methods very easily, since the master program just has to call the backward Euler routines with specific time step sizes and starting vectors.

Time adaptivity is obtained by using embedded methods as suggested in [2]. To this end, all stage derivatives are stored by the subsolvers. Then, the local error is estimated by the solvers separately, which then report the estimates back to the master program. Furthermore, if the possibility of rejected time steps is taken into account, the current solution pair $(\mathbf{u}, \mathbf{\Theta})$ has to be stored as well.

To comply with the condition that temperature and heat flux are continuous at the interface Γ, a so called Dirichlet-Neumann coupling is used. Namely, the boundary conditions for the two solvers are chosen such that we prescribe Neumann data for one solver and Dirichlet data for the other. Following the analysis of Giles [6], temperature is prescribed for the equation with smaller heat conductivity, here the fluid, and heat flux is given on Γ for the structure. Choosing the conditions the other way around leads to an unstable scheme.

In the following it is assumed that at time t_n, the step size Δt_n is prescribed. Applying a DIRK method to equation (6)-(7) results in the coupled system of equations to be solved at Runge-Kutta stage i:

$$\mathbf{F}(\mathbf{u}_i, \mathbf{\Theta}_i) := \mathbf{u}_i - \mathbf{s}_i^{\mathbf{u}} - \Delta t_n \, a_{ii} \underline{\mathbf{h}}(\mathbf{u}_i, \mathbf{\Theta}_i) = \mathbf{0}, \tag{8}$$

$$\mathbf{T}(\mathbf{u}_i, \mathbf{\Theta}_i) := [\mathbf{M} - \Delta t_n \, a_{ii} \mathbf{K}]\mathbf{\Theta}_i - \mathbf{M}\mathbf{s}_i^{\Theta} - \Delta t_n \, a_{ii} \bar{\mathbf{q}}(\mathbf{u}_i) = \mathbf{0}. \tag{9}$$

Here, $a_{ii} = 1 - \sqrt{2}/2$ is a coefficient of the time integration method and $\mathbf{s}_i^{\mathbf{u}}$ and $\mathbf{s}_i^{\Theta}$ are given vectors, called starting vectors, computed inside the DIRK scheme. The dependence of the fluid equations $\underline{\mathbf{h}}(\mathbf{u}_i, \mathbf{\Theta}_i)$ on the temperature $\mathbf{\Theta}_i$ results from the nodal temperatures of the structure at the interface. This subset is written as $\mathbf{\Theta}_i^{\Gamma}$. Accordingly, the structure equations depend only on the heat flux of the fluid at the coupling interface.

4 VECTOR EXTRAPOLATION

4.1 Basic fixed point iteration

To solve the coupled system of nonlinear equations (8)-(9), a strong coupling approach is employed. Thus, a nonlinear fixed point iteration is iterated until a convergence criterion is satisfied. In particular, we use a a nonlinear Gauß-Seidel process:

$$\mathbf{F}(\mathbf{u}_i^{(\nu+1)}, \mathbf{\Theta}_i^{(\nu)}) = \mathbf{0} \quad \rightsquigarrow \quad \mathbf{u}_i^{(\nu+1)} \tag{10}$$

$$\mathbf{T}(\mathbf{u}_i^{(\nu+1)}, \mathbf{\Theta}_i^{(\nu+1)}) = \mathbf{0} \quad \rightsquigarrow \quad \mathbf{\Theta}_i^{(\nu+1)}, \quad \nu = 0, 1, ... \tag{11}$$

Each solve is thereby done locally by the structure or the fluid solver. More specific, a Newton method is used in the structure and a FAS multigrid method is employed in the fluid.

The starting values of the iteration are given by $\mathbf{u}_i^{(0)} = \mathbf{s}_i^{\mathbf{u}}$ and $\mathbf{\Theta}_i^{(0)} = \mathbf{s}_i^{\Theta}$. The termination criterion is formulated by the nodal temperatures at the interface of the solid structure and we stop once we are below the tolerance in the time integration scheme divided by five.

$$\|\mathbf{\Theta}_i^{\Gamma\,(\nu+1)} - \mathbf{\Theta}_i^{\Gamma\,(\nu)}\| \leq TOL/5. \tag{12}$$

The vector

$$\mathbf{r}^{(\nu+1)} := \mathbf{\Theta}_i^{\Gamma\,(\nu+1)} - \mathbf{\Theta}_i^{\Gamma\,(\nu)} \tag{13}$$

is often referred to as the interface residual.

To improve the convergence speed of the fixed point iteration, different vector extrapolation techniques have been suggested. These are typically classic techniques, where a set of k vectors of a convergent vector sequence is extrapolated to obtain a faster converging sequence. We are now going to describe three techniques that we will test in this framework.

4.2 Aitken Relaxation

Relaxation means that after the fixed point iterate is computed, a relaxation step is added:

$$\tilde{\mathbf{\Theta}}_i^{\Gamma\,(\nu+1)} = \omega_{\nu+1}\mathbf{\Theta}_i^{\Gamma\,(\nu+1)} + (1-\omega_{\nu+1})\mathbf{\Theta}_i^{\Gamma\,(\nu)}. \tag{14}$$

Several strategies exist to compute the relaxation parameter ω.

The idea of Aitken's method is to enhance the current solution $\mathbf{\Theta}_i^{\Gamma\,(\nu+1)}$ using two previous iteration pairs $(\mathbf{\Theta}_i^{\Gamma\,(\nu+2)}, \mathbf{\Theta}_i^{\Gamma\,(\nu+1)})$ and $(\mathbf{\Theta}_i^{\Gamma\,(\nu+1)}, \mathbf{\Theta}_i^{\Gamma\,(\nu)})$ obtained from the Gauß-Seidel-Step (10)-(11). An improvement in the scalar case is given by the secant method

$$\tilde{\Theta}_i^{\Gamma\,(\nu+1)} = \frac{\Theta_i^{\Gamma\,(\nu-1)}\Theta_i^{\Gamma\,(\nu+1)} - \Theta_i^{\Gamma\,(\nu)}\Theta_i^{\Gamma\,(\nu)}}{\Theta_i^{\Gamma\,(\nu-1)} - \Theta_i^{\Gamma\,(\nu)} - \Theta_i^{\Gamma\,(\nu)} + \Theta_i^{\Gamma\,(\nu+1)}}. \tag{15}$$

The relaxation factor in equation (14) for the secant method (15) is then

$$\omega_{\nu+1} = \frac{\Theta_i^{\Gamma\,(\nu-1)} - \Theta_i^{\Gamma\,(\nu)}}{\Theta_i^{\Gamma\,(\nu-1)} - \Theta_i^{\Gamma\,(\nu)} - \Theta_i^{\Gamma\,(\nu)} + \Theta_i^{\Gamma\,(\nu+1)}}. \tag{16}$$

As customary, we use an added recursion on ω_i in which we use the old relaxation factor ω_ν:

$$\omega_{\nu+1} = -\omega_\nu \frac{r^{\Gamma\,(\nu)}}{r^{\Gamma\,(\nu+1)} - r^{\Gamma\,(\nu)}}. \tag{17}$$

In the vector case the division by residual $\mathbf{r}^{\Gamma\,(\nu+1)} - \mathbf{r}^{\Gamma\,(\nu)}$ is not possible. Therefore, we multiply nominator and numerator formally by $(\mathbf{r}^{\Gamma\,(\nu+1)} - \mathbf{r}^{\Gamma\,(\nu)})^T$ to obtain

$$\omega_{\nu+1} = -\omega_\nu \frac{(\mathbf{r}^{\Gamma\,(\nu)})^T(\mathbf{r}^{\Gamma\,(\nu+1)} - \mathbf{r}^{\Gamma\,(\nu)})}{\|\mathbf{r}^{\Gamma\,(\nu+1)} - \mathbf{r}^{\Gamma\,(\nu)}\|^2}. \tag{18}$$

Two previous steps are required to calculate the relaxation parameter. For the first fixpoint iteration, a relaxation parameter ν_1 is needed and therefore it must be prescribed.

4.3 Polynomial Vector Extrapolation

Another idea we will follow here are Minimal Polynomial Extrapolation (MPE) and Reduced Rank Extrapolation (RRE) [16]. Here, the new approximation is given as a linear combination of existing iterates with coefficients γ_ν to be determined:

$$\tilde{\mathbf{\Theta}}_i^{\Gamma\,(\nu+1)} = \sum_{j=0}^{\nu+1} \gamma_j \mathbf{\Theta}_i^{\Gamma\,j}. \tag{19}$$

For MPE, the coefficients are defined via

$$\gamma_j = \frac{c_j}{\sum_{i=0}^{\nu+1} c_i}, \quad j = 0, ..., \nu+1 \tag{20}$$

where the coefficients c_j are the solution of the problem

$$\min_{c_j} \left\| \sum_{j=0}^{\nu+1} c_j \mathbf{r}_j + \mathbf{r}_{\nu+1} \right\|_2. \tag{21}$$

For RRE, the coefficients are defined as the solution of the constrained least squares problem

$$\min_{\gamma_j} \left\| \sum_{j=0}^{\nu+1} \gamma_j \mathbf{r}_j \right\|_2, \quad \text{subject to} \sum_{j=0}^{\nu+1} \gamma_j = 1. \tag{22}$$

These problems are then solved using a QR decomposition.

5 NUMERICAL RESULTS

As a test case, the cooling of a flat plate resembling a simple work piece is considered. The work piece is initially at a much higher temperature than the fluid and then cooled by a constant air stream, see figure 1.

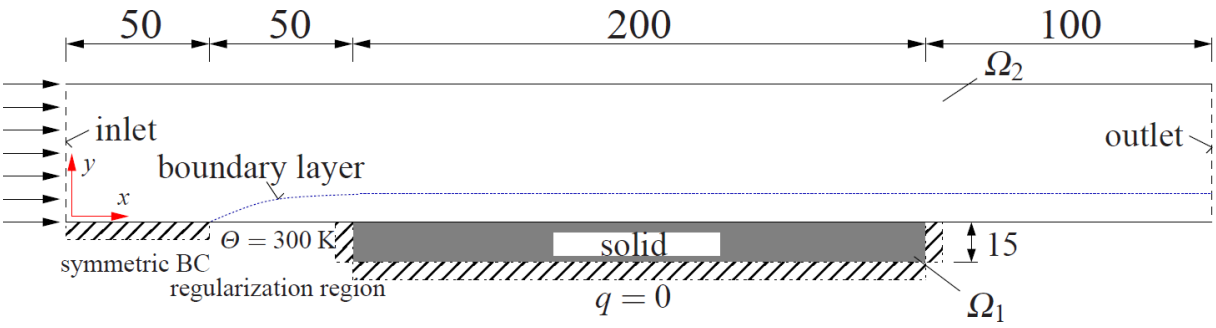

Figure 1: Test case for the coupling method

The inlet is given on the left, where air enters the domain with an initial velocity of $\mathrm{Ma}_\infty = 0.8$ in horizontal direction and a temperature of 273 K. Then, there are two succeeding regularization regions of 50 mm to obtain an unperturbed boundary layer. In the first region, $0 \leq x \leq 50$, symmetry boundary conditions, $v_y = 0$, $q = 0$, are applied. In the second region, $50 \leq x \leq 100$, a constant wall temperature of 300 K is specified. Within this region the velocity boundary layer fully develops. The third part is the solid (work piece) of length 200 mm, which exchanges heat with the fluid, but is assumed insulated otherwise, thus $q_b = 0$. Therefore, Neumann boundary conditions are applied throughout. Finally, the fluid domain is closed by a second regularization region of 100 mm with symmetry boundary conditions and the outlet.

Regarding the initial conditions in the structure, a constant temperature of 900 K at $t = 0$ s is chosen throughout. To specify reasonable initial conditions within the fluid, a steady state solution of the fluid with constant wall temperature $\Theta = 900$ K is computed.

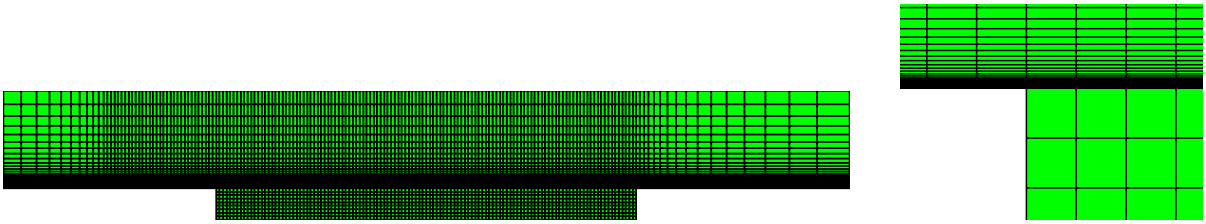

(a) Entire mesh (b) Mesh zoom

Figure 2: Full grid (left) and zoom into coupling region (right)

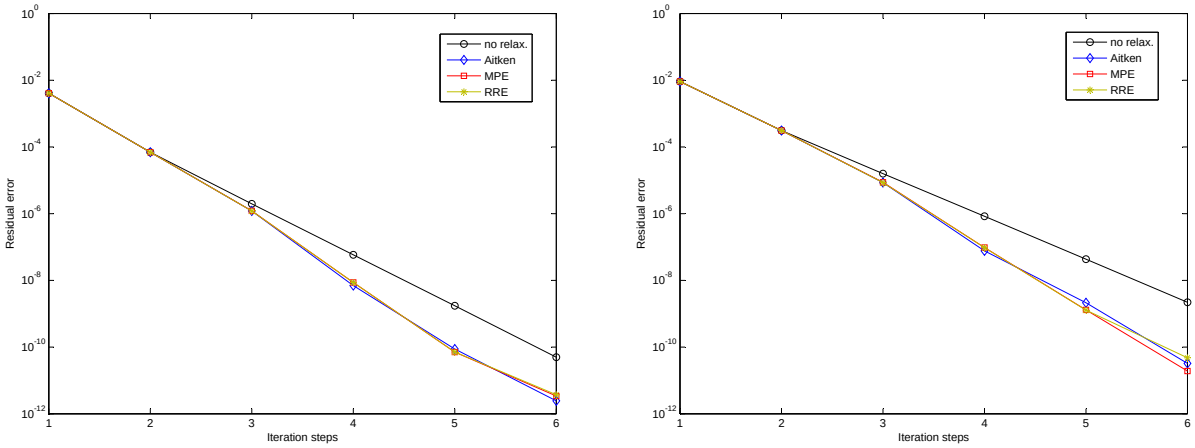

(a) 1 time step with a time step size of 1 s (b) 1 time step with a time step size of 5 s

Figure 3: Comparison of the relaxation methods for 1 time step with different timestep sizes

The grid is chosen cartesian and equidistant in the structural part, where in the fluid region the thinnest cells are on the boundary and then become coarser in y-direction (see figure 2). To avoid additional difficulties from interpolation, the points of the primary fluid grid, where the heat flux is located in the fluid solver, and the nodes of the structural grid are chosen to match on the interface Γ.

To compare the effect of the different relaxation strategies on one fixed point iteration, we consider the first stage of the first time step in the test problem with a time step size of $\Delta t = 1$s and $\Delta t = 5$s. In figure 3, we can see how the interface residual decreases with the fixed point iterations. During the first two steps all methods have the same residual norm. This is because all methods need at least two iterations to start. For this example, the extrapolation methods outperform the standard scheme for target residual norms below 10^{-5}.

We now compare the different schemes for a whole simulation of 100 seconds real time when we choose different tolerances TOL. When we use a time adaptive algorithm, a total number of eight time steps is needed to solve the test case problem in 100 seconds.

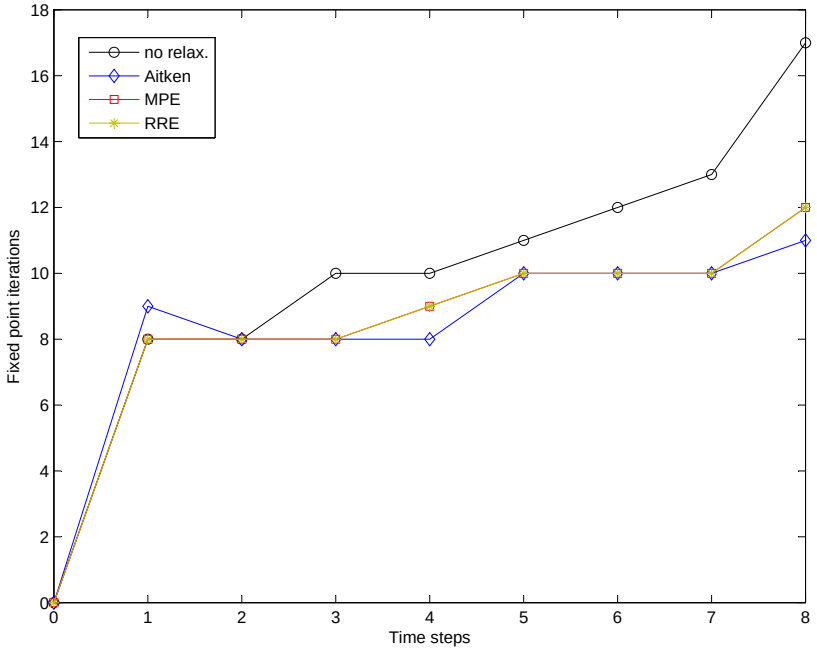

Figure 4: Number of fixed point iterations per time step

In figure 4, we see the number of fixed point iterations needed for each time step. The tolerance was chosen to be $TOL = 10^{-7}$. The dynamic relaxation methods needed a few less iterations. At the beginning of the time adaptive process, all of the methods started with the same time step size $\Delta t = 0.5$ s. With an increasing time and therefore an increasing time step size, caused by the adaptive algorithm, the normal (no relaxation) method needs more fixed point iterations in the end of that time interval, while the other methods have remained roughly constant. The total number of fixed point iterations is shown in tabular 1. As we can see, the extrapolation methods have an advantage over the normal (no relaxation) method for a tolerance of 10^{-7}. For $TOL = 10^{-4}$, all the methods need roughly the same number of iterations, which is also confirmed in Figure 3, where all methods overlap at 10^{-4}.

Table 1: Total number of iterations for 100 secs of real time

TOL		No relax.	Aitken	MPE	RRE
10^{-4}	#Iterations	53	48	50	50
10^{-7}	#Iterations	89	74	75	75

6 CONCLUSIONS

We considered a thermal fluid structure interaction problem where a nonlinear heat equation to model steel is coupled with the laminar compressible Navier-Stokes equations. The coupling is based on a Dirichlet-Neumann coupling. To obtain a fast solver, a higher order time adaptive method is used for time integration and different vector extrapolation techniques, namely Aitken Relaxation, MPE and RRE were compared for a test problem.

It turns out that for this simple problem, there is not much difference between the schemes for large tolerances, since the fixed point iteration terminates too quickly for the extrapolation schemes to make a difference. For tighter tolerances, the extrapolation schemes save 20% of iterations. Future work is on testing these schemes on more realistic examples.

REFERENCES

[1] A. L. Banka. Practical Applications of CFD in heat processing. *Heat Treating Progress*, (August), 2005.

[2] P. Birken, K. J. Quint, S. Hartmann, and A. Meister. A Time-Adaptive Fluid-Structure Interaction Method for Thermal Coupling. *Comp. Vis. in Science*, 13(7):331–340, 2011.

[3] J. M. Buchlin. Convective Heat Transfer and Infrared Thermography. *J. Appl. Fluid Mech.*, 3(1):55–62, 2010.

[4] C. Farhat. CFD-based Nonlinear Computational Aeroelasticity. In E. Stein, R. de Borst, and T. J. R. Hughes, editors, *Encyclopedia of Computational Mechanics*, volume 3: Fluids, chapter 13, pages 459–480. John Wiley & Sons, 2004.

[5] T. Gerhold, O. Friedrich, J. Evans, and M. Galle. Calculation of Complex Three-Dimensional Configurations Employing the DLR-TAU-Code. *AIAA Paper*, 97-0167, 1997.

[6] M. B. Giles. Stability Analysis of Numerical Interface Conditions in Fluid-Structure Thermal Analysis. *Int. J. Num. Meth. in Fluids*, 25:421–436, 1997.

[7] U. Heck, U. Fritsching, and K. Bauckhage. Fluid flow and heat transfer in gas jet quenching of a cylinder. *International Journal of Numerical Methods for Heat & Fluid Flow*, 11:36–49, 2001.

[8] M. Hinderks and R. Radespiel. Investigation of Hypersonic Gap Flow of a Reentry Nosecap with Consideration of Fluid Structure Interaction. *AIAA Paper*, 06-1111, 2006.

[9] U. Küttler and W. A. Wall. Fixed-point fluidstructure interaction solvers with dynamic relaxation. *Comput. Mech.*, 43:61–72, 2008.

[10] P. Le Tallec and J. Mouro. Fluid structure interaction with large structural displacements. *Comp. Meth. Appl. Mech. Engrg.*, 190:3039–3067, 2001.

[11] N. Lior. The cooling process in gas quenching. *J. Materials Processing Technology*, 155-156:1881–1888, 2004.

[12] R. C. Mehta. Numerical Computation of Heat Transfer on Reentry Capsules at Mach 5. *AIAA-Paper 2005-178*, 2005.

[13] C. Michler, E. H. van Brummelen, and R. de Borst. Error-amplification Analysis of Subiteration-Preconditioned GMRES for Fluid-Structure Interaction. *Comp. Meth. Appl. Mech. Eng.*, 195:2124–2148, 2006.

[14] K. J. Quint, S. Hartmann, S. Rothe, N. Saba, and K. Steinhoff. Experimental validation of high-order time integration for non-linear heat transfer problems. *Comput. Mech.*, 48(1):81–96, 2011.

[15] S. Schüttenberg, M. Hunkel, U. Fritsching, and H.-W. Zoch. Controlling of Distortion by means of Quenching in adapted Jet Fields. *Materialwissenschaft und Werkstofftechnik*, 37(1):92–96, 2006.

[16] A. Sidi. Review of two vector extrapolation methods of polynomial type with applications to large-scale problems. *J. Comp. Phys.*, 3(3):92–101, 2012.

[17] P. Stratton, I. Shedletsky, and M. Lee. Gas Quenching with Helium. *Solid State Phenomena*, 118:221–226, 2006.

[18] J. Vierendeels, L. Lanoye, J. Degroote, and P. Verdonck. Implicit Coupling of Partitioned Fluid-Structure Interaction Problems with Reduced Order Models. *Comp. & Struct.*, 85:970–976, 2007.

[19] U. Weidig, N. Saba, and K. Steinhoff. Massivumformprodukte mit funktional gradierten Eigenschaften durch eine differenzielle thermo-mechanische Prozessführung. *WT-Online*, pages 745–752, 2007.